

FIG. 3. Single-particle distribution function  $R(r)$  for solid  ${}^4\text{He}$  at two different volumes, as a function of the particle displacement from equilibrium  $r$ . The results of two different approximation methods are compared to one another and also to results from a Monte Carlo calculation.

ably well with experiment and with the MC results in the volume range shown, the comparison becomes increasingly unfavorable as the molar volume is decreased.

The single-particle-distribution function  $R(r)$  for  ${}^4\text{He}$ , at several different volumes, is shown on Fig. 3 as a function of the particle displacement from equilibrium  $r = |\vec{r}_i - \vec{R}_i|$ . The circles represent the results of the static-field approximation, from which it is evident that the atoms remain localized despite the fact that  $\beta = 0$  minimizes the energy. These results are compared with the MC results of Hansen and Levesque,<sup>1</sup> which are represented by the triangles. The values of  $\kappa$  which minimize the energy in the static-field approximation are larger than those derived from MC calculations.<sup>1,2</sup> This is understandable because, with  $\beta = 0$ , the various  $f(\vec{r}_i - \vec{R}_i)$  are entirely responsible for providing the localization necessitating a larger  $\kappa$  value.

As mentioned earlier, it is believed that the results of the static-field approximation are not

totally satisfactory because of the rigidity of the lattice of atoms providing the local field. The dynamical motion of an arbitrary atom  $\lambda$  is inhibited because the fixed atoms confine  $\lambda$  to a smaller effective volume than it would have if the atoms producing the local field were allowed to move in response to the motion. This situation apparently becomes more critical at higher pressure where the effective volume per atom is further reduced. McMahan<sup>13</sup> has recently calculated the exchange integral  $J$  for solid  ${}^3\text{He}$  by an approach that is apparently very similar to the static-field method. Although his results are reasonable at low pressure, they become increasingly unfavorable as the pressure increases. McMahan concludes as we do that the rigidity of the lattice is to blame and that this effect is more pronounced at higher densities.

The solution then is to properly describe the motion of the molecular-field atoms and the effect of this motion on all dynamical pairs  $(\lambda, \kappa)$ . The results of this dynamic-field approximation are now described.

#### B. Dynamic-field approximation

##### 1. ${}^3\text{He}$ data

Results for solid  ${}^3\text{He}$  are presented in Table I, where  $\langle T \rangle$  and  $\langle V \rangle$  are the expectation values of the kinetic and potential energies, respectively, and  $E_0$  is the total ground-state energy. The quantities  $\beta$  and  $\kappa$  are values of the variational parameters which minimize the energy and  $\langle r^2 \rangle^{1/2}$  is the root-mean-square atomic deviation from the equilibrium lattice site. Pressures and compressibilities are also tabulated. It should be kept in mind that all work on helium was done using a bcc lattice structure. Although the total energy, pressure, and compressibility do not differ significantly from one assumed lattice structure to another, the quantities  $\langle T \rangle$ ,  $\langle V \rangle$ , and  $\langle r^2 \rangle^{1/2}$  are somewhat more sensitive and any comparisons with other work must be made with this fact in mind.

Figure 1 shows the ground-state energy for  ${}^3\text{He}$  over the volume range  $19 \leq V \leq 24.5$  cm<sup>3</sup>/mole. The

TABLE I. bcc  ${}^3\text{He}$  results.

Volume (cm <sup>3</sup> /mole)	$\langle V \rangle$ (K)	$\langle T \rangle$ (K)	$E_0$ (K)	Pressure (atm)	Compressibility (10 <sup>4</sup> atm <sup>-1</sup> )	$\langle r^2 \rangle^{1/2}$ A	$\beta$ ( $\sigma^{-2}$ )	$\kappa$ ( $\sigma^{-1}$ )
24.50	-22.19	21.94	-0.25			1.18	3.6	1.11
20.80	-26.98	28.38	1.40	50	23.8	1.06	4.1	1.11
16.16	-32.31	41.12	8.81	260	7.0	0.85	6.5	1.08
14.00	-32.21	51.43	19.22	565	3.9	0.75	8.7	1.06
11.82	-24.76	69.70	44.94	1380	1.8	0.62	12.5	1.04
10.25	-8.30	92.25	83.95	2820	0.7	0.52	19.0	1.02

circles represent experimental data,<sup>12</sup> the triangles are the MC results of Hansen and Levesque,<sup>1</sup> and the inverted triangles are the MC results of Hansen and Pollock.<sup>2</sup> The solid line represents the dynamic-field results, the dotted line is the static-field results, and the dashed line represents the theory of Horner.<sup>14</sup> A sample comparison of our calculated energy and that of Hansen and Levesque at  $V=24.3$  cm<sup>3</sup>/mole is  $E=0.21$  and  $0.63$  K, respectively. Similarly, at  $V=19.12$  cm<sup>3</sup>/mole, the comparison is  $E=4.01$  and  $4.07$  K, respectively. It is interesting to observe that results of the two MC calculations differ from one another by amounts that are significantly outside the statistical error quoted in either article. There are, however, modest differences in the two calculations which could account for this fluctuation. The dynamic-field approximation requires the evaluation of a nine-dimensional integral. These integrals have been evaluated with sufficient accuracy to conservatively guarantee the resulting energy values to within  $\sim 3\%$ . In view of the fluctuation in the MC results we conclude that they and the dynamic-field results are in agreement. The energy minimizing values for  $\beta$  and  $\kappa$ , listed in Table I, also compare well with the MC results, unlike the values derived from the static-field approximation. Figure 4 shows the ground-state energy over a greater volume range  $10 \leq V \leq 24.5$  cm<sup>3</sup>/mole. A sample comparison of our calculated energy with that of Hansen and Pollock at  $V=11.17$  cm<sup>3</sup>/mole gives  $E=54.17$  and  $52.5$  K, respectively. We observe, as do Hansen and Pollock, that the energy falls below the experimental values at low volumes. This is attributed to the inexact description of the pair interaction provided by the Lennard-Jones 6-12 potential.<sup>5</sup> Figure 5 shows the pressure-volume (PV) relationship and, in Fig. 6, is the single-particle distribution function  $R(r)$  for six different volumes. These data are tabulated in Tables I and II. The compressibility is shown in Fig. 7 and compared with experiment over the

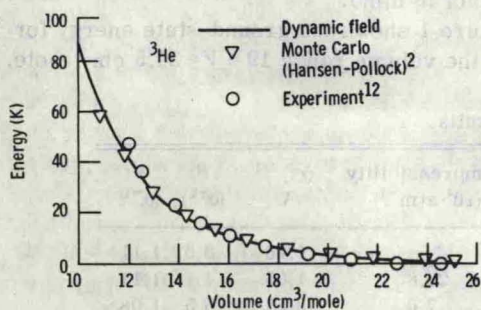


FIG. 4. Energy vs volume for solid <sup>3</sup>He over the volume range  $10 < V \leq 24.5$  cm<sup>3</sup>/mole. A comparison is made with other theoretical work and experiment.

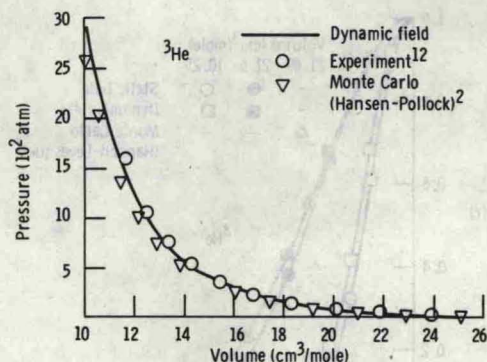


FIG. 5. Pressure vs volume for solid <sup>3</sup>He. A comparison is made with other theoretical work and experiment.

volume range  $10 \leq V \leq 24.5$  cm<sup>3</sup>/mole. These results are substantially more uncertain than the energy because they involve a second derivative of the energy with respect to the volume.

## 2. <sup>4</sup>He results

The calculated data for solid <sup>4</sup>He are presented in Table III. Figure 2 shows the ground-state energy over the volume range  $16 \leq V \leq 21.65$  cm<sup>3</sup>/mole. Similarly, Fig. 8 shows the energy over a greater volume range  $10 \leq V \leq 21.65$  cm<sup>3</sup>/mole. The experimental data<sup>12</sup> and other theoretical results are presented with the same format as Figs. 1 and 4 for <sup>3</sup>He. A sample comparison of our calculated energy and that of Hansen and Levesque at  $V=21.49$  cm<sup>3</sup>/mole is  $E=-5.14$  and  $-5.17$  K, respectively. Similarly, at  $V=17.08$  cm<sup>3</sup>/mole, the comparison is  $E=-2.63$  and  $-2.39$  K, respectively. A comparison with Hansen and Pollock's

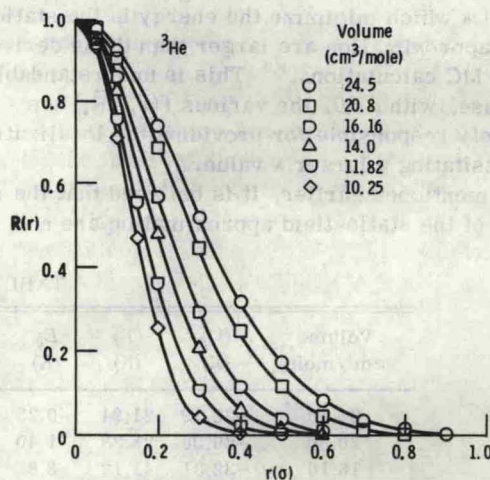


FIG. 6. Single-particle distribution function  $R(r)$  vs particle displacement from equilibrium for solid <sup>3</sup>He at various volumes.